Proc. NIPR Symp. Upper Atmos. Phys., 2, 84–95, 1989

GEOS-1 OBSERVATION OF HISS-TRIGGERED CHORUS EMISSIONS IN THE OUTER MAGNETOSPHERE AND THEIR GENERATION MODEL

Katsumi HATTORI[1], Masashi HAYAKAWA[1], Shin SHIMAKURA[2], Michel PARROT[3] and François LEFEUVRE[3]

[1]*Research Institute of Atmospherics, Nagoya University, 13, Honohara 3-chome, Toyokawa 442*
[2]*Department of Electrical and Electronic Engineering, Faculty of Engineering, Chiba University, 33, Yayoi 1-chome, Chiba 260*
[3]*Laboratoire de Physique et Chimie de l'Environnement, CNRS, 45071 Orleans Cedex 2, France*

Abstract: The co-existence of hiss and chorus is frequently observed on board satellites in the outer magnetosphere, and chorus emissions are observed in the data from GEOS-1 satellite to start nearly at the uppermost frequency of the hiss band. The direction finding measurements have been made for these hiss-triggered chorus events. On the basis of the direction finding results and detailed analysis of the fine structures in the hiss band, we have suggested a generation model how a chorus is triggered by a hiss such that some coherent wavelets near the top of the hiss band phase-bunch electrons at the equator, and these phase-bunched electrons radiate a coherent signal as they move away from the equator. Also, theoretical computations have been carried out in order to explain the df/dt, θ value (the polar angle between the wave normal direction and the Earth's magnetic field) and other factors by means of a two-dimensional ray-tracing method. The differences between the experimental and theoretical values are pointed out, and some possibilities to remedy these discrepancies are discussed.

1. Introduction

The wave phenomena and wave-particle interaction processes in the outer magnetosphere have been investigated from the standpoints of both geophysics and plasma physics. Among the fundamental and unsolved problems connected with plasma physics in the outer magnetospheric plasma, one of the greatest concern is to know the connection between two types of magnetospheric VLF/ELF emissions (hiss (CORNILLEAU-WEHRLIN *et al.*, 1978; HAYAKAWA *et al.*, 1986a, b, c) and chorus (BURTIS and HELLIWELL, 1976; GOLDSTEIN and TSURUTANI, 1984; HAYAKAWA *et al.*, 1984)), in particular whether or not these two are essentially different. The phenomenon suitable for this study is "hiss-triggered chorus". Two different mechanisms have been suggested so far for triggering a chorus. The one attributes it to hiss which is considered to be incoherent and turbulent, because the previous satellite and ground observations have indicated that a chorus is often accompanied by a background hiss (BURTIS and HELLIWELL, 1976; CORNILLEAU-WEHRLIN *et al.*, 1978; KOONS, 1981), although chorus is, on many occasions, spontaneously generated. Another pos-

sible stimulus to trigger a chorus is pointed out by LUETTE *et al.* (1977) to be a power line harmonic radiation, and they have concluded that man-made VLF noise such as a power line radiation plays an important role in triggering chorus, although this hypothesis has been questioned by TSURUTANI *et al.* (1979). We will study this problem by means of many hiss-triggered chorus events observed by GEOS-1 satellite.

The wave data observed on board GEOS-1 satellite were utilized to examine the wave characteristics (the rate of frequency increase, the dependence of chorus triggering rate on the hiss intensity etc.) of hiss-triggered chorus events and then we calculated the wave normal directions of hiss and chorus emissions by means of wave distribution function direction finding measurements. On the basis of these experimental results, we will present a model how a chorus is triggered by hiss.

2. Wave Characteristics of Hiss-Triggered Chorus and the Wave Normals of Hiss and Chorus

The field data are signals obtained by the so-called S-300 experiment on board GEOS-1 satellite, which measures continuously the electric and magnetic field components of the wave field (S-300 EXPERIMENTERS, 1979). The observed signals are subjected to onboard analyses; the swept frequency analyzers (SFA's) and a correlator. Six SFA's which may be operated with any sensor combination, have a bandwidth of 300 Hz and are swept in frequency in the range 0–77 kHz. Before being telemetered onto the ground, the signals are transposed in frequency, passed through identical low-pass filters at 450 Hz and sampled at 1.488 kHz. A spectral matrix composed of the mean auto-power and cross-power spectra among the multiple field components at each Fourier component is estimated by using the magnetic SFA data. In the present paper we use the direction finding measurement based on the wave distribution function (LEFEUVRE *et al.*, 1981; HAYAKAWA *et al.*, 1986a) in order to know the wave normal directions, not only for chorus but also for hiss.

The observation of hiss-triggered chorus is made on the satellite during the period of about 30 minutes from 1212 to 1241 UT on 21st July, 1977, at an L value of 6.5–6.7, at geomagnetic latitude from 6.8 to 8.5 and LT$\simeq$13 h. A few sonagrams in the ELF band (0–2.5 kHz) are selected and illustrated in Fig. 1. As seen from Fig. 1(a), a lot of chorus elements are seen to appear from an intense hiss band. The chorus is intensified compared with the hiss band, and the starting frequency of a chorus is asymptotic to the hiss band, and this feature indicates obviously that hiss is the cause and chorus is an effect therefrom or a consequence. Although the hiss in Fig. 1(b) looks stronger than in Fig. 1(a), the actual hiss intensity is about one order of magnitude smaller than that in Fig. 1(a); hence we can find no chorus triggering. A study of the relationship between the chorus triggering rate and the hiss intensity has indicated that there exists a threshold hiss power, only above which a significant chorus triggering is expected (power threshold effect).

The starting frequency of chorus emission seen in Fig. 1 is about 0.9 kHz and the final frequency is about 1.6 kHz. The duration of a chorus element is about 1.0 s, and the rate of frequency increase df/dt, in linear fit, of chorus elements is found

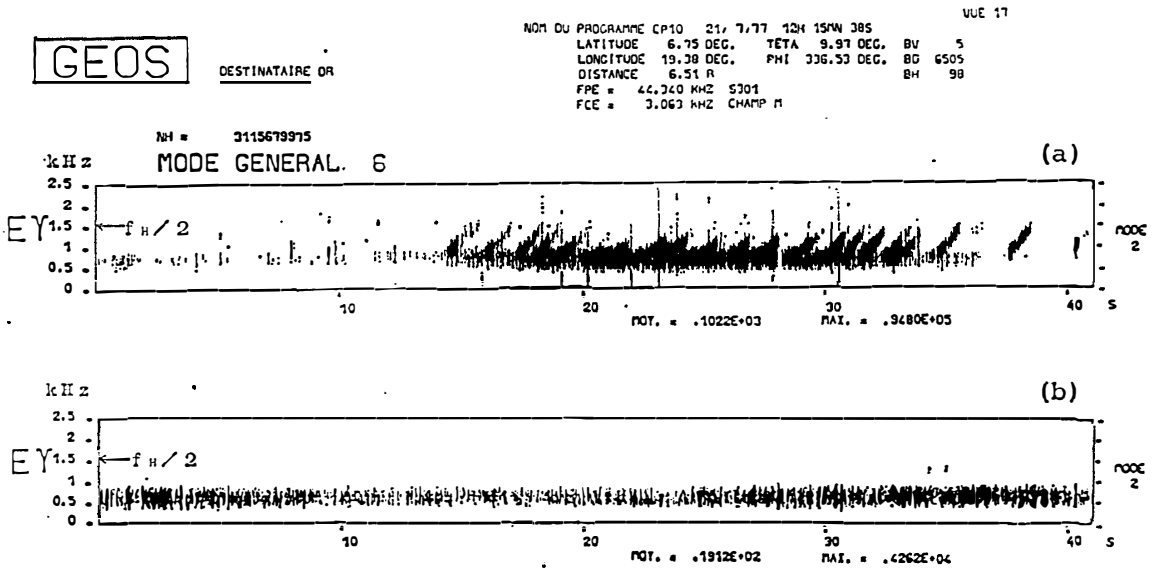

Fig. 1. A few examples of the spectrograms of hiss-triggered chorus emissions observed on board GEOS-1 satellite.

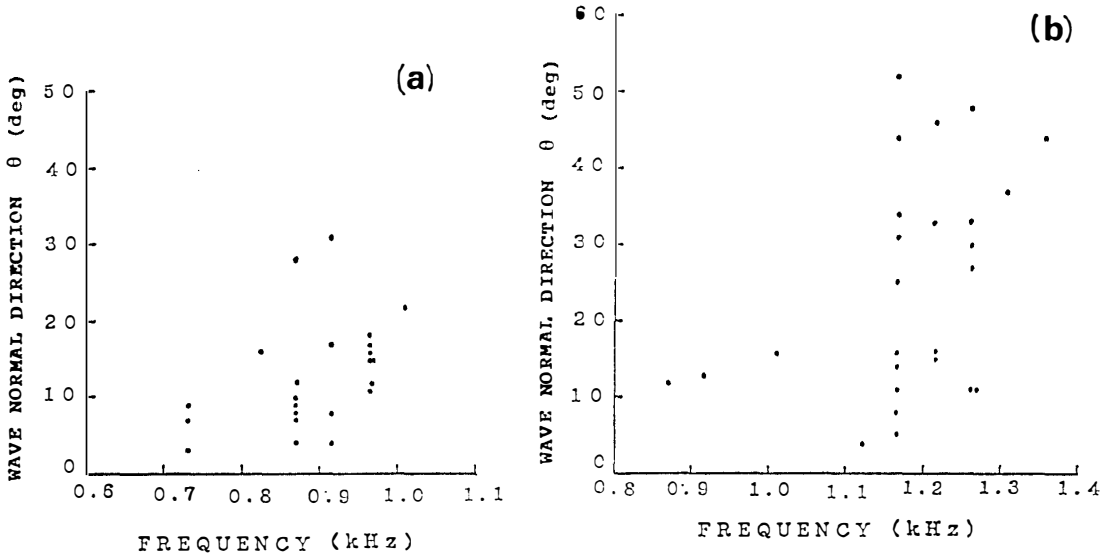

Fig. 2. Direction finding results of hiss (a) and chorus (b). The wave normal angle (θ) with respect to the magnetic field is plotted as a function of frequency.

to be around 0.7 kHz/s, which seems to be a typical value at these L values and at these LT's (BURTIS and HELLIWELL, 1976).

The measurements to determine the wave normal directions of the causative hiss and resultant chorus have been performed and Fig. 2 is their result. It is understood from this diagram that the hiss emissions make small angles less than 30° with the magnetic field, or rather we find a high concentration of $\theta < 20°$, which means that the hiss propagates approximately along the magnetic field. On the other hand, the characteristics of wave normals of chorus in Fig. 2(b) are very different from those of hiss. At relatively lower frequency, θ is found to be smaller than 15°, but

we find a greater scatter at higher frequency (>1.6 kHz). There are two distinct groups in θ values; one is a smaller θ group with θ less than 15°, and the other is a larger θ group ($25° < \theta < 55°$). The azimuthal angles of wave normals are located within 60° from the magnetic meridian plane.

Next we discuss the fine structures within the hiss band. Detailed spectral analyses by means of maximum entropy method have yielded an occasional occurrence of monochromatic coherent wavelets within the hiss band, and their duration is tens of milliseconds (TSUJI *et al.*, 1989). It is quite reasonable to suppose that the intensity of such coherent wavelets is also enhanced in correspondence with the average intensity of hiss over a certain bandwidth (48 Hz) used. These coherent wavelets in the upper side of the hiss band are supposed to phase-bunch resonant electrons in the vicinity of the equator. Figure 3 illustrates the intensity of hiss observed on board GEOS-1 satellite, which is the intensity averaged over a certain bandwidth (48 Hz). In order to estimate the reasonableness of phase-bunching by coherent wavelets in the hiss band, we calculate the phase-bunching time (HELLIWELL, 1970), and Fig. 4 shows the dependence of the phase-bunching time on the magnetic intensity of hiss. If we take a bandwidth of 4 Hz for the coherent wavelets, and we take the most probable value from Fig. 3, the phase-bunching time (Tb) (HELLIWELL, 1967, 1970; KOONS, 1981) is found to be shorter than 10 ms, because the hiss intensity in the present paper is very high when we take into account the intensity range of VLF emissions as observed in HELLIWELL (1970). On the other hand, the wave-particle interaction time (Tr) which is calculated based on the inhomogeneity of medium (HELLIWELL, 1967; SCHULZ, 1972), is 100 ms (and the intrinsic bandwidth due to inhomogeneity around the equator (SCHULZ, 1972; KOONS, 1981) is 10–20 Hz). When we compare Tb with Tr, it is found that Tb is much shorter

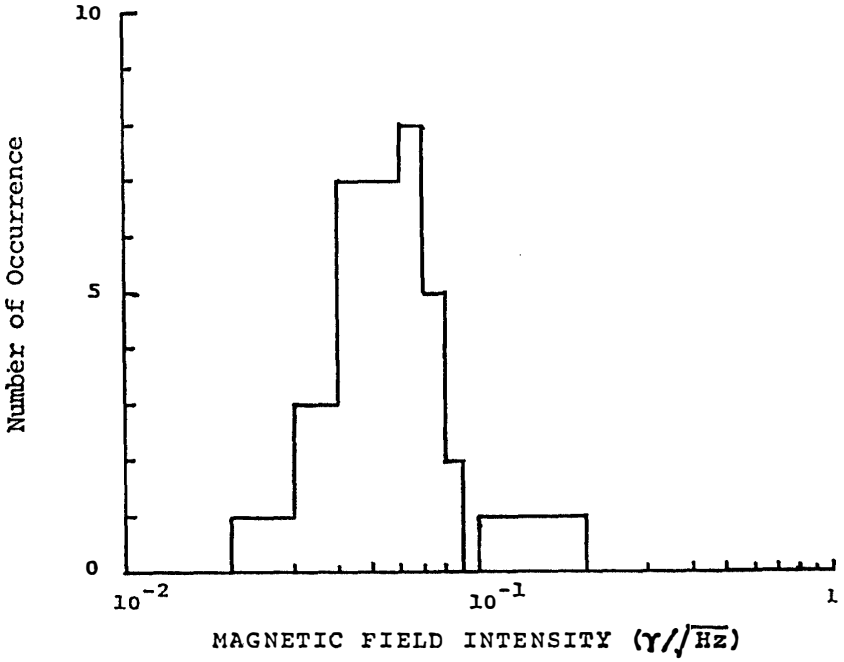

Fig. 3. The occurrence histogram of the average hiss intensity.

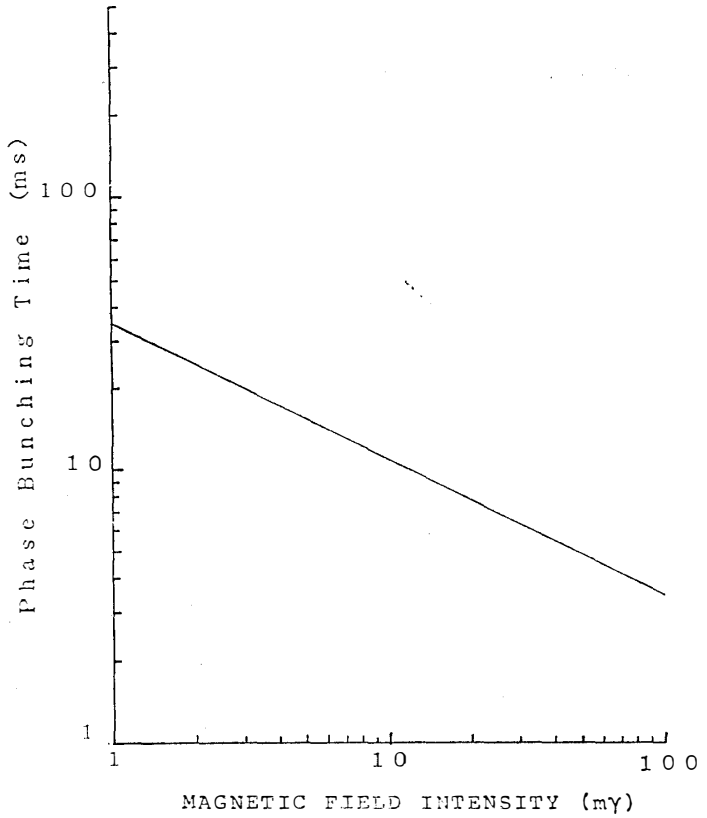

Fig. 4. The relationship between the phase-bunching time (Tb) and magnetic field intensity of hiss.

than Tr. Therefore, some coherent wavelets near the top of the hiss band are able to phase-bunch the electrons at the equator. The large difference of the rate of chorus triggering in Fig. 1 can be explained in terms of the difference in the intensity of the causative hiss, because very weak hiss in Fig. 1(b) is unable to phase-bunch the electrons, leading to no chorus triggering.

3. Generation Mechanism of Hiss-Triggered Chorus

Based on the observational features mentioned in the previous section, we can draw the following scenario on how a chorus is triggered from the hiss band. Hiss is so far considered to be incoherent and turbulent. But this is not true, and we understand that monochromatic and coherent wavelets or local maxima near the upper edge of the hiss band can be found on many occasions. These coherent wavelets might be related with the theoretical prediction by NUNN (1986), who suggested from his computer simulation on the wave-particle interaction in an intense band-limited hiss that some nonlinear wave-particle interaction might cause a broad-band spectrum to fragment into narrow-band forms. As discussed in the previous section on the basis of a detailed consideration of phase-bunching time using the measured intensity, the interaction time due to the inhomogeneity around the equator, intrinsic bandwidth, and so on, such coherent wavelets are strong enough to phase-

bunch the electrons at the equator. The hiss was also found to propagate along the magnetic field according to the results of direction findings, and this condition is very preferable for an effective phase-bunching. As these electrons phase-bunched in the vicinity of the equator, move adiabatically away from the equator along the field line, they radiate, toward the equator, a Doppler-shifted coherent wave which satisfies the cyclotron resonance condition and the dispersion relation, resulting in the detection of a chorus at the satellite. The emission frequency is shown as a function of emission latitude in Fig. 5. Chorus is assumed to be generated at each latitude with $\theta=0°$, which seems to be supported experimentally by the direction finding for chorus at normalized frequency below 0.3 (HAYAKAWA *et al.*, 1984; GOLDSTEIN and TSURUTANI, 1984). The subsequent propagation in two different modes (ducted and non-ducted) are considered here. For the non-ducted propagation we carry out a two-dimensional ray-tracing computation because the observed azimuthal values were found to be rather close to the magnetic meridian plane as mentioned before. The shape of a chorus is determined by the time delay as a function of frequency computed as the sum of the travel time for the electrons phase-bunched initially at the equator to move to the emission latitude plus the group delay time of the emission from the emission latitude to the satellite. The dynamic spectra theoretically predicted for the above two propagation modes are shown in Fig. 6 for a specific equatorial pitch angle ($\alpha_{eq}=45°$) of the resonant electrons, which fits best with the experimental one as in Fig. 1.

It is found from Fig. 6 that the theoretical df/dt is 1.08 kHz/s for ducted propagation and 0.80 kHz/s for non-ducted propagation. The same calculations were carried out for resonant electrons with different equatorial pitch angles, and Table 1 summarizes those results for the df/dt. In these computations, we adopted a dif-

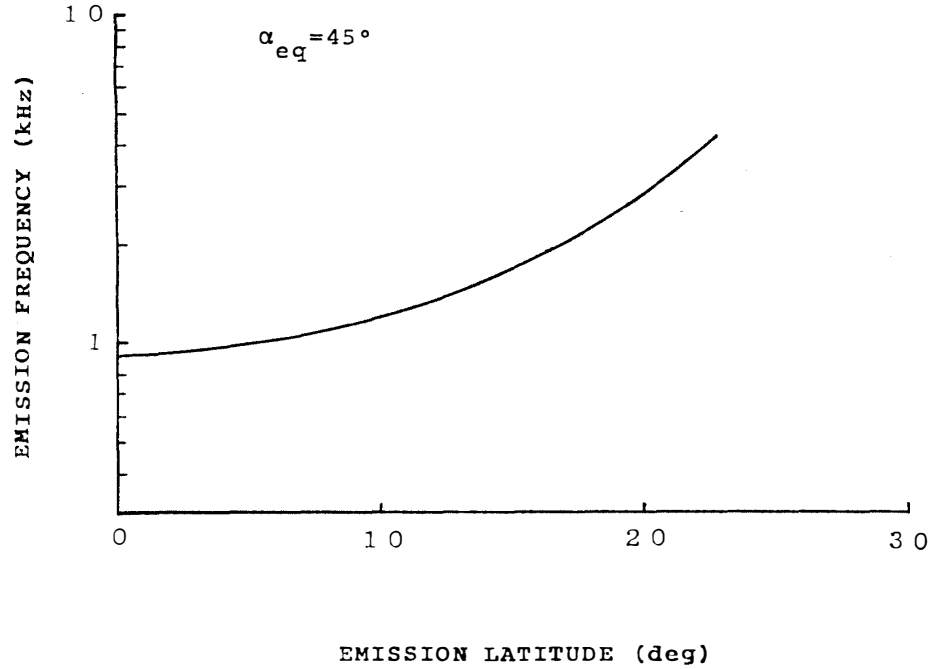

Fig. 5. The relationship between the emission frequency and emission latitude.

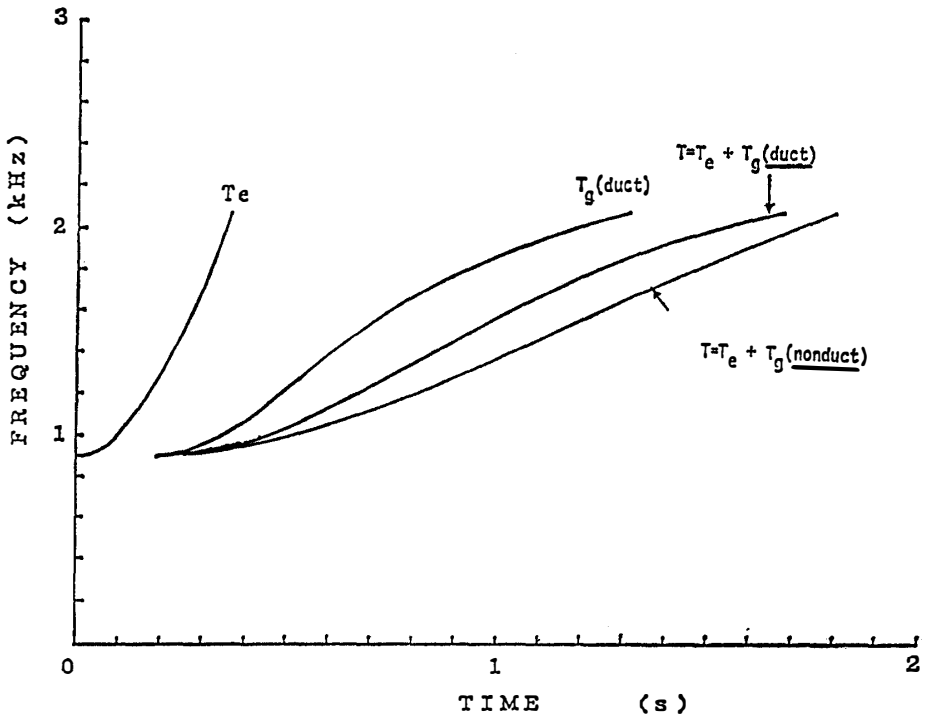

Fig. 6. The theoretically predicted dynamic spectra of chorus emissions. T_e is the time during which the electrons phase-bunched at the equator, travel to the emission region, and T_g is the time delay during which the emitted wave propagates back to the satellite.

fusive equilibrium model for the plasma density and a dipole model for the magnetic field, such that the equatorial value along the geomagnetic field line of $L=6.67$ of gyrofrequency and plasma frequency are 2.853 kHz and 19.2 kHz, respectively. The longitudinal energy of resonant electrons with equatorial pitch angle 45° is found to be about 5.5 keV and the total energy is 10.9 keV.

Table 1 indicates that as equatorial pitch angle increases, the value of df/dt becomes smaller. The df/dt observed on board GEOS-1 satellite was about 0.7 kHz/s, and when we compare the observed value with these theoretical ones in Table 1, non-ducted propagation seems more acceptable than ducted propagation, and the case of $\alpha_{eq}=30°$ seems to show the best fit.

As for the non-ducted mode, we discuss theoretically two other important wave behaviors; one is the variation of θ at the satellite location with emission latitude, and the other is the deviation of rays at the satellite latitude from the initial L value on which waves are emitted. Figure 7 illustrates that the theoretically obtained value of θ at the satellite position is larger than 35°, and this is greatly different from the direction finding results in Fig. 2. Figure 8 demonstrates the geocentric distance of rays at the satellite latitude as a function of the emission latitude, and the broken line indicates the actual satellite geocentric distance. This figure shows that for higher emission latitude (correspondingly higher frequency), it is more difficult to detect the emission at the satellite. Judging from these considerations, we have to think of the following factors to resolve the above discrepancies; (1) an extent in L value of the generation region, (2) the emission angle is not $\theta=0°$, and (3) a

Table 1. The theoretical values of df/dt (in kHz/s) with different equatorial pitch angles in the case of ducted and non-ducted propagation modes.

Equatorial pitch angle α_{eq}	Ducted propagation	Non-ducted propagation
30°	0.93	0.72
45°	1.08	0.80
60°	1.13	1.07

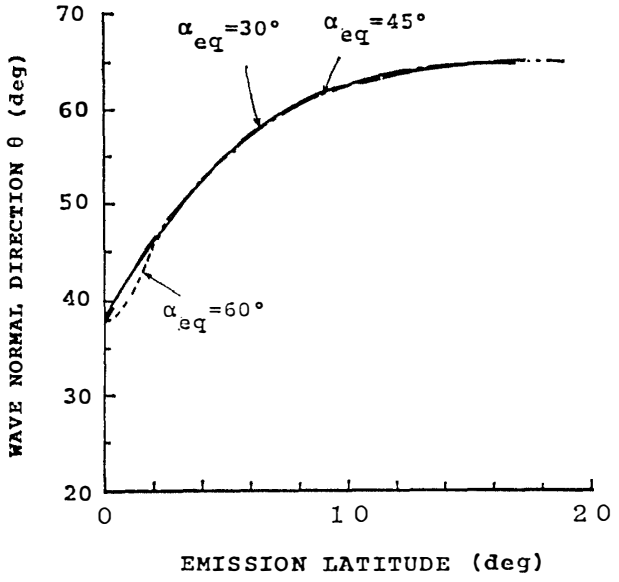

Fig. 7. The wave normal direction (θ) at the satellite latitude as a function of emission latitude in the case of non-ducted propagation.

combination of ducted and non-ducted propagation modes. These three conditions or factors are briefly discussed below. Although condition (1) must be taken into account in the generation model, the computation results are not found to remedy the discrepancy concerning the θ value at the satellite latitude in the case of emission generated with $\theta=0°$, and the obtained df/dt is found to exhibit a greater difference from the observation. Therefore, even if factor (1) really exists, it is not a dominant factor.

Next we consider the influence of condition (2). It has been pointed out that the waves at the normalized frequencies below 0.3 are generated at $\theta\sim0°$ (HAYAKAWA *et al.*, 1984; GOLDSTEIN and TSURUTANI, 1984). However, GOLDSTEIN and TSURUTANI (1984) suggested that it seems likely that chorus is generated near the Gendrin angle (θ_g) at the normalized frequencies above 0.3. The frequency range we are dealing with in this paper, lies in a range from 0.3 to 0.43 of normalized frequencies, and so it may be possible to assume the oblique instability at θ_g. We take some characteristic emission angles and the ray tracing results are shown in Fig. 9 as a function of emitted frequency. We understand that these results correspond to the frequency dependence of θ value of an individual chorus element at the satellite latitude. In Fig. 10 we paid attention to the frequency dependence in Fig. 2 of individual chorus elements, and a line connecting a few dots belongs to one chorus element. This diagram is based on Fig. 2. A comparison of Figs. 9 and 10 yields

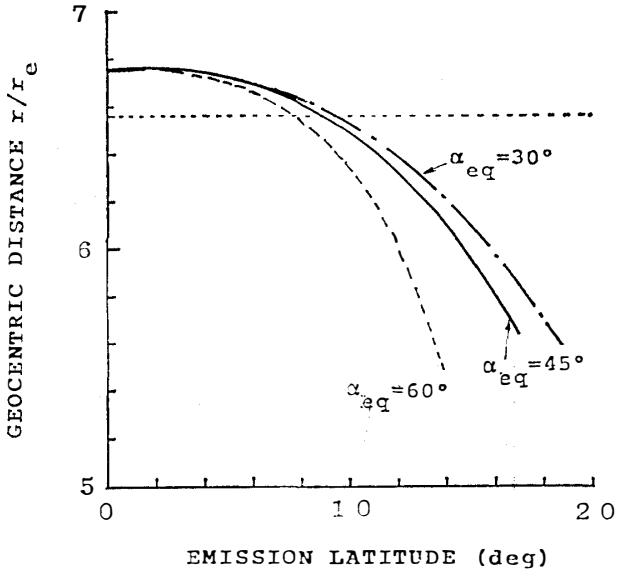

Fig. 8. The geocentric distance (r/r_e r_e: Earth's radius)) at the satellite latitude as a function of emission frequency in the case of non-ducted propagation. The broken line indicates the satellite geocentric distance.

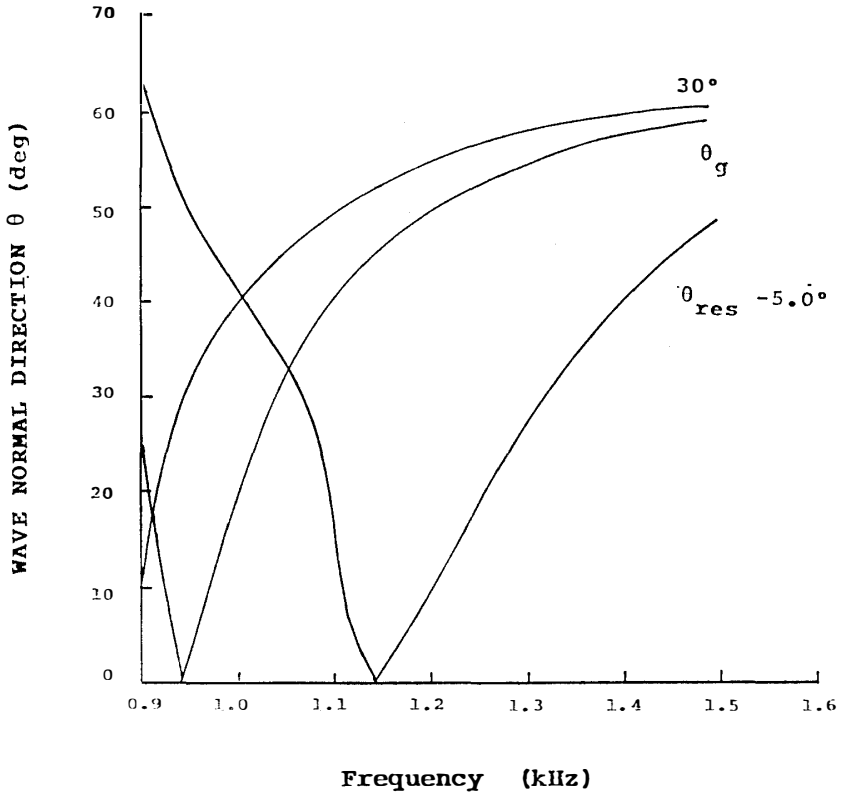

Fig. 9. The theoretical variation of θ at the satellite in the case of non-ducted propagation with the wave generation with wave normals at θ_g and $\theta_{res}-5.0$, together with the case of wave generation angle $\theta=30°$.

that most of the observed θ values seem to exist within the theoretical curves corresponding to θ_g and $\theta_{res}-5.0°$ (θ_{res}: oblique resonance angle). Unfortunately we do not have a complete set of direction finding results over individual chorus elements, and so that we cannot reach any definite conclusion for this effect. However, the

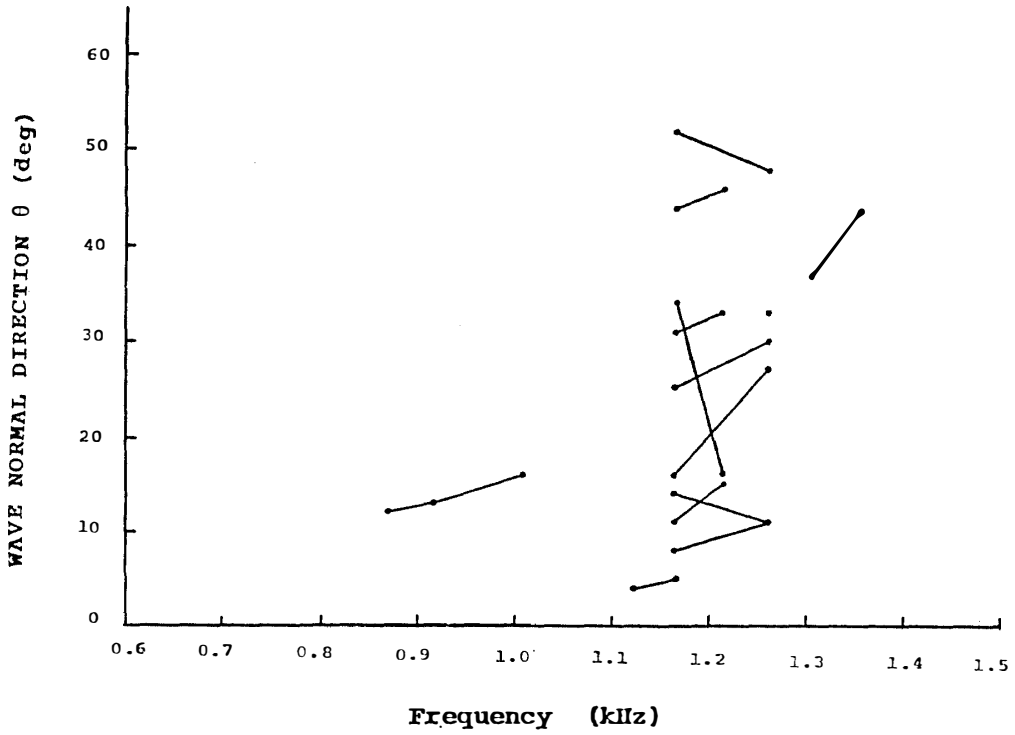

Fig. 10. The re-arrangement of Fig. 2(b) in the form of frequency dependence of θ for individual chorus elements.

observed θ dependence at the satellite is rather well explained and also the df/dt seems to be quite similar to the observation.

Finally, we discuss factor (3). It is very convenient to explain with this factor the statistical results of direction findings shown in Fig. 2, *i.e.*, the smaller θ group less than 30° is the consequence of the ducted propagation, and a larger θ group more than 30° is attributed to the non-ducted propagation as given in Fig. 7. Although we discussed these possible factors or conditions, we cannot say definitely which one of them is more dominant than any others, and further observational studies are required.

4. Conclusion

We studied the mechanism of hiss-triggered chorus emissions in the outer magnetosphere observed on board GEOS-1 satellite and a detailed description of observational results and the physical implications will be published elsewhere. The process of hiss-triggered chorus is composed of the following two stages. There are occasionally monochromatic and coherent wavelets in the preexisting hiss band, whose duration is tens of milliseconds. Those wavelets in the hiss band are found to propagate along the geomagnetic field line and those in the vicinity of the upper edge of the hiss band are found to be able to phase-bunch the resonant electrons at the equator. Then, as the phase-bunched electrons move away from the equatorial plane, they radiate Doppler-shifted coherent waves toward the equator due to the coherent cyclotron instability.

The important characteristics to be studied are the df/dt and wave normal direction (θ). In the present paper we paid attention to the difference of these values between the observation and theoretical prediction, and we suggest three possibilities to reduce these differences. We found that two possibilities among the three seem to be more important; one concerns with the emission angle of waves and the other is the co-existence of ducted and non-ducted propagation modes.

Unfortunately, we cannot point out definitely which factor is most significant. We present a general scenario of hiss-triggered chorus based on the GEOS-1 satellite data, but there remain many unsolved finer problems in this scenario. We can list the following important future experiments so as to obtain a very definite story of hiss-triggered chorus. (1) The fine structures in the hiss band should be investigated by means of a sophisticated spectral analysis with high resolution. Also, we have to trace the coherent wavelets in the hiss band and then to trace the frequency and intensity of the subsequent chorus, which would be of great importance in the microphysics of hiss-triggered chorus. (2) In order to reduce the discrepancy concerning the wave normal angle and df/dt (especially wave normal angle) and to resolve the problems raised in this paper, further extensive studies should be carried on the basis of the data from the equatorial and off-equatorial observations, and, in these studies, the direction finding would be of great importance. The comparison of the characteristics obtained in this paper with those at different latitudes would provide us with significant information. (3) In the proposed scenario, we assumed that the interaction region moves with the participating electrons and this is an extreme case of the drifting oscillator model of HELLIWELL (1967). The comparison of the wave characteristics (bandwidth, df/dt, θ value etc.) at different latitudes will provide useful information whether this model is acceptable or the generalization by HELLIWELL (1967) is required. Also, the wave normals other than 0° will be investigated. These studies are all in progress, and we will report on these subjects in the near future.

References

BURTIS, W. J. and HELLIWELL, R. A. (1976): Magnetospheric chorus; Occurrence patterns and normalized frequency. Planet. Space Sci., **24**, 1007–1024.

CORNILLEAU-WEHRLIN, N., GENDRIN, R., LEFEUVRE, F., PARROT, M., GRARD, R., JONES, D., BAHNSEN, A., UNGSTRUP, E. and GIBBONS, W. G. (1978): VLF waves observed onboard GEOS-1. Space Sci. Rev., **22**, 371–382.

GOLDSTEIN, B. E. and TSURUTANI, B. T. (1984): Wave normal directions of chorus near the equatorial source region. J. Geophys. Res., **89**, 2789–2810.

HAYAKAWA, M., YAMANAKA, Y., PARROT, M. and LEFEUVRE, F. (1984): The wave normals of magnetospheric chorus emissions observed on board GEOS-2. J. Geophys. Res., **89**, 2811–2821.

HAYAKAWA, M., OHMI, N., PARROT, M. and LEFEUVRE, F. (1986a): Direction finding of ELF hiss in a detached plasma region of the magnetosphere. J. Geophys. Res., **91**, 135–141.

HAYAKAWA, M., TANAKA, Y., SAZHIN, S. S., OKADA, T. and KURITA, K. (1986b): Characteristics of dawnside mid-latitude VLF emissions associated with substorms as deduced from the two-stationed direction finding measurement. Planet. Space Sci., **34**, 225–243.

HAYAKAWA, M., TANAKA, Y., SHIMAKURA, S. and IIZUKA, A. (1986c): Statistical characteristics of medium-latitude VLF emissions (unstructured and structured); The local time dependence and the association with geomagnetic disturbances. Planet. Space Sci., **34**, 1361–

1372.

HELLIWELL, R. A. (1967): A theory of discrete VLF emissions from magnetosphere. J. Geophys. Res., **72**, 4773–4790.

HELLIWELL, R. A. (1970): Intensity of discrete VLF emissions. Particles and Fields in the Magnetosphere, ed. by B. M. MCCORMAC. Dordrecht, Reidel, 292.

KOONS, H. C. (1981): The role of hiss in magnetospheric chorus emissions. J. Geophys. Res., **91**, 6745–6754.

LEFEUVRE, F., PARROT, M. and DELANNOY, C. (1981): Wave distribution functions estimation of VLF electromagnetic waves. J. Geophys. Res., **86**, 2359–2375.

LUETTE, J. P., PARK, C. G. and HELLIWELL, R. A. (1977): Longitudinal variations of very low frequency chorus activity in the magnetosphere; Evidence of excitation by electrical power transmission lines. Geophys. Res. Lett., **4**, 275–278.

NUNN, D. (1986): A nonlinear theory of sideband stability in ducted whistler mode waves. Planet. Space Sci., **34**, 429–451.

SCHULZ, M. (1972): Intrinsic bandwidth of cyclotron resonance in the geomagnetic field. Phys. Fluids, **15**, 2448–2449.

S-300 EXPERIMENTERS (1979): Measurements of electric and magnetic wave fields and of cold plasma parameters onboard GEOS-1. Preliminary results. Planet. Space Sci., **27**, 317–359.

TSUJI, S., HAYAKAWA, M., SHIMAKURA, S. and HATTORI, K. (1989): On the statistical properties of magnetospheric ELF/VLF hiss. Proc. NIPR Symp. Upper Atmos. Phys., **2**, 74–83.

TSURUTANI, B. T., SMITH, E. J., CHURCH, J. R., THORNE, R. M. and HOLZER, R. E. (1979): Does ELF chorus show evidence of power line stimulation? Wave Instabilities in Space Plasma, ed. by P. J. PALMADESSO and K. PAPADOULOS. Dordrecht, D. Reidel, 51–54.

(Received November 1, 1988; Revised manuscript received January 11, 1989)